A Full-Wave Phase Aberration Correction Method for Transcranial High-Intensity Focused Ultrasound Brain Therapies

Scott Almquist-*IEEE Member*, Joshua de Bever-*IEEE Member*, Robb Merrill, Dennis Parker, and Douglas Christensen-*IEEE Life Member*

***Abstract*— Transcranial high-intensity focused ultrasound has recently been used to noninvasively treat several types of brain disorders. However, due to the large differences in acoustic properties of skulls and the surrounding soft tissue, it can be a challenge to adequately focus an ultrasonic beam through the skull. We present a novel, fast, full-wave method of correcting the aberrations caused by the skull by phasing the elements of a phased-array transducer to create constructive interference at the target. Because the method is full-wave, it also allows for trajectory planning by determining the phases required for multiple target points with negligible additional computational costs. Experimental hydrophone scans with an *ex vivo* skull sample using a 256-element 1-MHz transducer show an improvement of 6.2% in peak pressure at the focus and a reduction of side-lobe pressure by a factor of 2.31. Additionally, mispositioning of the peak pressure from the intended treatment location is reduced from 2.3 to 0.5 mm.**

I. Introduction

High-intensity focused ultrasound (HIFU) is emerging as a promising treatment modality for many diseases. Focused ultrasound beams offer target treatment in a noninvasive manner using no ionizing radiation. Often, the treatment is guided using MRI-based temperature imaging (MRgFUS). Of particular interest is transcranial focused ultrasound, which may be used in ablation of tumors [1], treatment of essential tremors [2], targeted drug delivery [3], neurostimulation [4], and several other diseases [5].

In many HIFU applications, inhomogeneous tissues can cause aberrations in the beam pattern that can lead to diffused and shifted focal locations, and may introduce significant energy in side lobes away from the primary focus – preventing effective treatment. These aberrations can be a problem for some soft tissue treatments when a large-aperture transducer is used [6], but the effects are much more prominent in transcranial treatments due to the large differences in acoustic properties of the skull and surrounding soft tissues.

*Research supported by NIH grant 5R01EB013433-03 and by the Focused Ultrasound Surgery Foundation.

S. Almquist is with the Department of Computer Science, University of Utah, Salt Lake City, UT 84112 USA (e-mail: scott.almquist@utah.edu).

J. de Bever is with Department of Computer Science, University of Utah, Salt Lake City, UT 84112 USA (e-mail: jdebever@cs.utah.edu).

R. Merrill is with the Utah Center for Advanced Imaging Research, University of Utah, Salt Lake City, UT 84112 USA (e-mail: merrobb@yahoo.com).

D. Parker is with the Utah Center for Advanced Imaging Research, University of Utah, Salt Lake City, UT 84112 USA (e-mail: parker@ucair.med.utah.edu).

D. Christensen is with the Department of Electrical & Computer Engineering and the Department of Bioengineering, University of Utah, Salt Lake City, UT 84112 USA (e-mail: christen@ee.utah.edu).

Numerous methods of phase correction have been developed [7]. These methods are based on varying the element phases of a phased-array transducer such that maximum constructive interference is achieved at the intended treatment location. Implantable hydrophones [8] offer the best possible corrections, but are invasive. Using cavitation to create shock waves that can be imaged ("ultrasonic stars" [9]) is noninvasive, but the energy required to create cavitation and the bubbles themselves may pose a risk to the patient. Methods based on MR acoustic radiation force imaging [10] can avoid cavitation, but may require more time to converge to the correct phases. All of these methods require increased table time for calibration. This extra time is exacerbated for the large element-number arrays used in transcranial treatments to prevent unwanted heating at the skull surface.

Simulation-based methods offer the benefit of being noninvasive, having no increased ultrasonic energy being deposited, and no increased MR table time. Often these simulations utilize geometric and bone density information about the skull gained from a CT scan. Assumptions are made to map the CT Hounsfield Units (HU) to acoustic properties such as density, attenuation and speed of sound. Previous finite-difference time-domain (FDTD) simulations based on CT scans [11] took about two hours to compute corrections. Faster simulations can be achieved by simplifying the acoustic models [12]; however, this will result in reduced focus intensity. A more detailed review of phase correction methods can be found in [7].

In this paper, we present a full-wave simulation-based method of correcting for phase aberrations introduced by the skull. The method is noninvasive, requires no increased MR table time, and can be used to correct for multiple treatment locations with no additional computational cost.

II. Methods

A. Simulation Technique

This phase aberration correction method employs simulations obtained with the Hybrid Angular Spectrum (HAS) method [13]. HAS works by alternating between the space and spatial-frequency domains to simulate 3D ultrasonic beam patterns that take into account refraction, reflection, and absorption. The benefit of using the HAS technique comes from the computational speed increase over other simulation methods (often two orders of magnitude faster than FDTD calculations).

For phase correction, HAS is used to calculate the 3D pressure patterns for each individual element of the phased-array transducer, initially assuming zero phase and uniform

978-1-4244-7929-0/14/$26.00 ©2014 IEEE

amplitude. Phase offsets can then be determined by taking the negative of the phase from each element at the desired focal location. When impressed on the individual elements, this results in maximum constructive interference at the desired point in the simulated volume. Various treatment locations can be handled by saving the phases over the entire possible treatment volume. Since HAS is already calculating the complex pressure for these points, there is negligible additional computational cost for multiple treatment sites.

To speed up simulations, computations for each element are performed in parallel on a Nvidia Tesla GPU (Nvidia, Santa Clara, CA). The simulations can be performed in a relatively short period of time. For small models (229 x 159 x 182 voxels with six tissue types) the computations can be completed in approximately 45 seconds. Larger models, such as the one used in the experimental portion of this work (421 x 648 x 170 voxels with 3000 distinct bone types), take approximately 15 minutes to compute.

B. Experimental Methods

Verification of the phase correction method was performed using an *ex vivo* section of human skull and a 1-MHz 256-element phased-array transducer (Imasonic, Besançon, France) driven by high-power generators (IGT, Bordeaux, France). The skull was cleaned and frozen for several weeks before being imaged in a custom holder in a CT scanner at 0.46 x 0.46 x 0.3-mm resolution. The holder was designed to provide a flat surface at a measured distance from the transducer in a tank of degassed water, with mounting holes that allowed it to be held at a known fixed rotation angle relative to the transducer.

A hydrophone (Onda HNR-0500, Onda Corporation, Sunnyvale, CA) was scanned in a raster pattern in the transverse plane at the geometric focus using two stepper motors (Thorlabs NRT150, Thorlabs Inc, Newton, New Jersey). Pressure scans were performed at a resolution of 0.25 mm covering an area 15 x15 mm.

For purposes of phase aberration correction, speed of sound is the most important acoustic parameter to be found by the procedure described next. Density for the inner and outer bone tables was set at 1.9 g/cm^3 while the diploë was set at 1.7 g/cm^3. The attenuation was set at 0.23 and 2.3 Np/(cm·MHz) for the tables and diploë respectively. These values correspond with typical literature values [14]. The demarcation between the skull tables and diploë was set at 707 HU, based on [15].

Acoustic models were built by linearly mapping the measured CT Hounsfield Units to speed-of-sound values (truncated to a minimum speed of sound of 1500 m/s). A similar linear speed-of-sound model has been validated in previous research [16]. In order to obtain the parameters for the best fit of the linear model (slope and intercept) to experimental data, experimental hydrophone scans were compared to simulated hydrophone scans, and the following metric was minimized:

$$\min \sum (p_{exp} - p_{sim})^2,$$

where p_{exp} is the pressure at each point obtained by the hydrophone scans, p_{sim} is the pressure at the same point from simulations, and the summation is over the 2D plane of focus. The minimization was computed using the Nelder-Mead simplex method [17] provided through MATLAB's (MathWorks, Natick, MA) *fminsearch* optimization function.

Acoustic models with the values obtained above were then used to generate corrected phases on a Nvida Tesla GPU using MATLAB code and the Jacket library (AccelerEyes, Atlanta, GA). Hydrophone scans were performed with the target at the geometric focus of the transducer with no skull in place, and with the skull in place, both with and without phase correction.

III. Results

The minimization mapping of HU to speed-of-sound values (c) resulted in the following formula:

$$c = 2.85(HU) + 1160,$$

with a minimum c of 1500 m/s. A representative slice of the resulting speed-of-sound pattern in the skull flap is shown in Fig. 1.

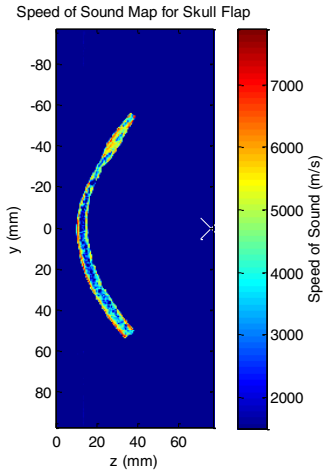

Figure 1. Representative slice of speed-of-sound values (m/s) in the skull flap obtained by the optimization routine. The transducer is to the left of the image with the beam propagating to the right focusing at the point indicated by a white X.

Based upon HAS calculations to obtain the phase correction values for each element, Fig. 2 shows the generated phases for each transducer element as well as the element locations on the transducer face.

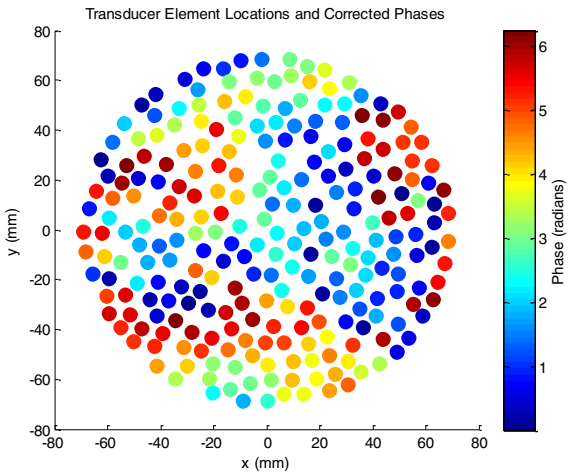

Figure 2. Transducer element locations and computed corrected phases for targeting through the skull to the geometric focus.

Fig. 3 shows the pressure patterns from the hydrophone scans without the skull in place (water only), with the skull in place but no corrections, and with the skull in place with phase corrections. The intended target point was at the graph origin (i.e., at the geometric focus) for both scans shown without phase correction; however, due to an even number of voxels in the y-direction for the phase corrected method, the intended target is shifted down 0.46 mm from the graph origin.

The phase correction method resulted in a 6.2% increase in peak pressure (13% increase in intensity) compared to the uncorrected method. Phase correction additionally reduced the misregistration distance of the point of highest pressure from the intended treatment location from 2.3 mm to 0.5 mm. Furthermore, the highest pressure in any side lobe was reduced by a factor of 2.31 after phase correction. It should further be noted that these results understate the benefit of phase correction since the total output power in the phase corrected case is reduced compared to the uncorrected case as a result of electrical cross-talk in the transducer system that occurs between elements of differing phases.

IV. Conclusion

Our method of phase correction is both fast and effective. Computation of phase correction values for large models (421 x 648 x 170 voxels) can be achieved in 15 minutes. Although the corrected pressure pattern is still not as tight at the focus as with no skull in place, the phase correction method increased peak pressure by at least 6%, reduced the misregistration distance to the intended target location, and reduced the side-lobe pressure, despite a decrease in acoustic output power due to electrical cross-talk in the transducer setup.

The phase correction abilities of the method are heavily dependent the accuracy of acoustic model. Future work will involve investigating the accuracy and repeatability of generating linear acoustic models from CT scans as well as other non-CT methods of creating models.

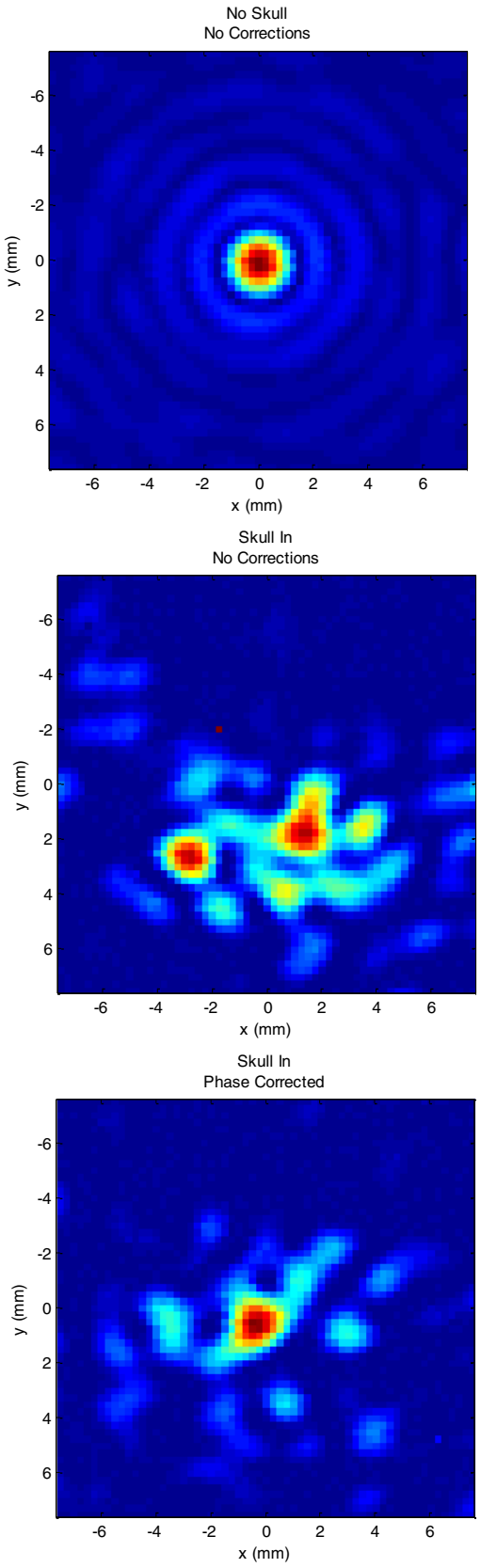

Figure 3. Hydrophone pressure-pattern scans with no skull in place (water only, top), skull in place with no aberration correction (middle), and skull in place with phase correction (bottom). Both scans with the skull in place are normalized to the same scale.

Although not shown here, the method generates full 3D pressure patterns, so multiple treatment locations are possible. The ability to generate treatment trajectories is important when treating large volumes, such as tumors. It may also be possible to use 3D pressure patterns to predict or prevent unwanted heating, especially on the skull surface where much of the ultrasound energy is deposited.

REFERENCES

[1] N. McDannold, G. Clement, P. Black, F. Jolesz, and K. Hynynen, "Transcranial MRI-guided focused ultrasound surgery of brain tumors: Initial findings in three patients," *Neurosurgery*, vol. 66, no. 2, pp. 323–332, Feb. 2010.

[2] W. J. Elias, D. Huss, T. Voss, J. Loomba, M. Khaled, E. Zadicario, R. C. Frysinger, S. A. Sperling, S. Wylie, S. J. Monteith, J. Druzgal, B. B. Shah, M. Harrison, and M. Wintermark, "A Pilot Study of Focused Ultrasound Thalamotomy for Essential Tremor," *N. Engl. J. Med.*, vol. 369, no. 7, pp. 640–648, 2013.

[3] Kullervo Hynynen, Nathan McDannold, Natalia Vykhodtseva, Scott Raymond, Ralph Weissleder, Ferenc A. Jolesz, and Nickolai Sheikov, "Focal disruption of the blood–brain barrier due to 260-kHz ultrasound bursts: a method for molecular imaging and targeted drug delivery," *http://dx.doi.org/10.3171/jns.2006.105.3.445*, 20-Jul-2007. [Online]. Available: http://thejns.org/doi/abs/10.3171/jns.2006.105.3.445?prevSearch=focal%2Bdisruption%2Bof%2Bthe%2Bblood%2Bbrain%2Bbarrier&searchHistoryKey=. [Accessed: 06-Jan-2014].

[4] R. L. King, J. R. Brown, W. T. Newsome, and K. B. Pauly, "Effective Parameters for Ultrasound-Induced In Vivo Neurostimulation," *Ultrasound Med. Biol.*, vol. 39, no. 2, pp. 312–331, Feb. 2013.

[5] S. Monteith, J. Sheehan, R. Medel, M. Wintermark, M. Eames, J. Snell, N. F. Kassell, and W. J. Elias, "Potential intracranial applications of magnetic resonance–guided focused ultrasound surgery: A review," *J. Neurosurg.*, vol. 118, no. 2, pp. 215–221, Feb. 2013.

[6] C. Mougenot, M. Tillander, J. Koskela, M. O. Köhler, C. Moonen, and M. Ries, "High intensity focused ultrasound with large aperture transducers: A MRI based focal point correction for tissue heterogeneity," *Med. Phys.*, vol. 39, no. 4, pp. 1936–1945, Mar. 2012.

[7] G. T. Clement and K. Hynynen, "Micro-receiver guided transcranial beam steering," *IEEE Trans. Ultrason. Ferroelectr. Freq. Control*, vol. 49, no. 4, pp. 447–453, Apr. 2002.

[8] M. Pernot, G. Montaldo, M. Tanter, and M. Fink, "'Ultrasonic stars' for time-reversal focusing using induced cavitation bubbles," *Appl. Phys. Lett.*, vol. 88, no. 3, p. 034102, Jan. 2006.

[9] U. Vyas, E. Kaye, and K. B. Pauly, "Transcranial phase aberration correction using beam simulations and MR-ARFI," *Med. Phys.*, vol. 41, no. 3, p. 032901, Feb. 2014.

[10] F. Marquet, M. Pernot, J.-F. Aubry, G. Montaldo, L. Marsac, M. Tanter, and M. Fink, "Non-invasive transcranial ultrasound therapy based on a 3D CT scan: protocol validation and in vitro results," *Phys. Med. Biol.*, vol. 54, no. 9, p. 2597, May 2009.

[11] G. T. Clement and K. Hynynen, "Correlation of ultrasound phase with physical skull properties," *Ultrasound Med. Biol.*, vol. 28, no. 5, pp. 617–624, May 2002.

[12] A. Kyriakou, E. Neufeld, B. Werner, M. M. Paulides, G. Szekely, and N. Kuster, "A review of numerical and experimental compensation techniques for skull-induced phase aberrations in transcranial focused ultrasound," *Int. J. Hyperthermia*, vol. 30, no. 1, pp. 36–46, Feb. 2014.

[13] U. Vyas and D. Christensen, "Ultrasound beam simulations in inhomogeneous tissue geometries using the hybrid angular spectrum method," *IEEE Trans. Ultrason. Ferroelectr. Freq. Control*, vol. 59, no. 6, pp. 1093–1100, 2012.

[14] F. J. Fry and J. E. Barger, "Acoustical properties of the human skull," *J. Acoust. Soc. Am.*, vol. 63, no. 5, pp. 1576–1590, May 1978.

[15] M. R. Norton and C. Gamble, "Bone classification: an objective scale of bone density using the computerized tomography scan," *Clin. Oral Implants Res.*, vol. 12, no. 1, pp. 79–84, 2001.

[16] J.-F. Aubry, M. Tanter, M. Pernot, J.-L. Thomas, and M. Fink, "Experimental demonstration of noninvasive transskull adaptive focusing based on prior computed tomography scans," *J. Acoust. Soc. Am.*, vol. 113, no. 1, pp. 84–93, Jan. 2003.

[17] J. C. Lagarias, J. A. Reeds, M. H. Wright, and P. E. Wright, "Convergence Properties of the Nelder--Mead Simplex Method in Low Dimensions," *SIAM J. Optim.*, vol. 9, no. 1, pp. 112–147, Jan. 1998.